Critical heat flux in locally heated liquid film moving under the action of gas flow in a mini-channel

E M Tkachenko[1,2], D V Zaitsev[1], E V Orlik[1] and O A Kabov[1,3]

[1]Kutateladze Institute of Thermophysics SB RAS, 1 Lavrentyev Ave., Novosibirsk 630090, Russia
[2]Novosibirsk State University, 2 Pirogova Str., Novosibirsk 630090, Russia
[3]Tomsk Polytechnic University, 30 Lenin Ave., Tomsk 634050, Russia

Corresponding author: egor_tkachenko@mail.ru

Abstract. Thin and ultra thin liquid films driven by a forced gas/vapor flow (stratified or annular flows), i.e. shear-driven liquid films in a narrow channel, is one of the promising candidate for the thermal management of advanced semiconductor devices with high local heat release. In experiments performed in this paper with locally heated shear-driven liquid films of water the effect of various conditions, such as flow rates of liquid and gas and channel height, on critical heat flux (CHF) was investigated. In experiments the record value of CHF as high as 540 W/cm^2 has been achieved. The heat spreading into the substrate and the heat loses into the atmosphere in total don't exceed 30% at heat fluxes higher than 200 W/cm^2. Comparison of shear-driven liquid films and gravity-driven liquid films showed that CHF in shear-driven films up to 10 times higher than in gravity-driven liquid films. Thus, prospect of using shear-driven films of water in modern cooling systems of semiconductor devices was confirmed.

1. Introduction

The development of modern microelectronic equipment requires efficient cooling systems. Increasing performance demands have resulted in greater non-uniformity of on-chip power dissipation, creating localized, "hot spots," often exceeding 1 kW/cm^2 in heat flux, which can degrade the processor performance and reliability [1]. Ultra thin liquid films driven by a forced gas/vapor flow in the mini-channel are promising for the use in thermal control systems of modern semiconductor devices [2]. Works [3-5] are devoted to analytical and numerical study of hydrodynamics and heat and mass transfer during joint motion of intensively evaporating liquid film and gas flow in minichannels. Authors of experimental works [6-8] established the basic laws of the flow and crisis phenomena in the liquid film moving under the action of the gas flow in the horizontal channel. First experiments with locally heated shear-driven liquid films have revealed that contrary to gravity-driven liquid films, shear-driven films are less likely to rupture. This provides a way to prevent and control hot dry patch formation by the shear stress induced by the gas flow. Disruption of the liquid film and formation of dry patches is important for the understanding of crisis phenomena in liquid films [9-11]. The main goal of the present work is to study rupture and CHF in locally heated shear-driven liquid films at heat fluxes higher than 500 W/cm^2. Also in this paper the data on heat loses into the atmosphere and heat spreading into the substrate are presented.

2. Experimental setup

Schematic of the test section is presented in figure 1. The main part of the test section is a thin stainless steel plate with a flush-mounted copper rod. At the working surface the rod has a 1×1 cm square head emulating surface of a computer chip. The rod is heated by a heating spiral coiled around its lower part. Such construction of the heater provides the condition at the heater surface T = const (which is confirmed by thermocouples measurements). The test section is covered with a transparent cover made of optical glass so that a flat channel is formed. We used six different channel heights, namely: 0.25, 0.5, 1, 1.2, 1.5 and 2.0 mm. Gas, pumped by a compressor, flows through the channel and passes to the atmosphere at the end of the test section. The liquid is supplied from a thermostat, gets into the channel through a liquid nozzle and flows under the friction of the gas along the stainless steel plate as a film. The liquid is accumulating at the bottom part of the test section and is returned into the thermostat. Distance from the gas inlet to the liquid nozzle is 57 mm and distance from the liquid nozzle to the heater is 32 mm. This provides steady flows of gas and liquid at the moment they reach the heater. Channel width is 40 mm. Several thermocouples are embedded in the stainless steel plate and in the copper rod, allowing determination of the working surface temperature. The temperature of the heater surface is calculated taking into account the depth at which the thermocouples are embedded (2 mm). All the thermocouples are individually calibrated to an accuracy of 0.1°C. The test section is oriented horizontally. When investigating liquid films falling under the action of gravity the test section is set vertically while the glass cover is removed.

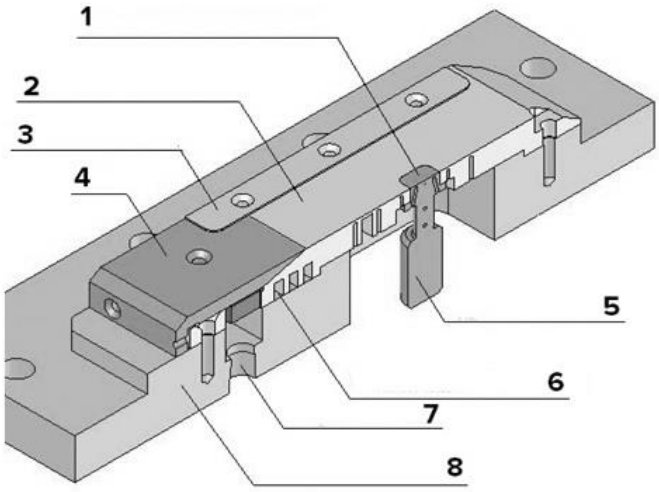

Figure 1. Design of test section: 1- source of the local heating; 2- stainless steel plate; 3- channel height control; 4- knife; 5- copper rod; 6- thermostabilizer; 7- liquid inlet; 8- textollite substrate.

Distilled water with initial temperature of 24°C is used as the working liquid. Air with temperature of 24-27 °C and relative humidity of 15-30% is used as the working gas. The experiments are carried out under stationary conditions. Superficial gas velocity (volumetric gas flow rate divided by cross-sectional area of the channel) U_{Sg} varies from 0.1 to 40 m/s.

The heat flux is determined by the electrical power dissipated on the heating spiral. Figure 2 presents data on the heat loses into the atmosphere and heat spreading into the steel plate. Thermal conductivity of copper is 400 W/mK which is almost 30 times higher than that of stainless steel (15 W/mK). This provides moderate heat spreading from the heater to the stainless steel plate: about 15% at q>200 W/cm^2, about 20% at q=100 W/cm^2 and up to 30% for smaller heat fluxes (according to estimation using measurements of thermocouples embedded into the stainless steel plate) (figure 2). Heat spreading into the atmosphere has been calculated as the ratio of the heat flux between two thermocouples embedded into the copper rod (estimated by measurements of thermocouples) and the

total heat flux determined by the electrical power. In order to minimize heat spreading from the heating spiral into the atmosphere, the heating spiral is wrapped with a layer of heat insulation material (mineral wool). Heat loses into the atmosphere don't exceed 15-20% (figure 2). Thus, the heat loses into the atmosphere and heat spreading into the steel plate in total don't exceed 30% at heat fluxes higher than 200 W/cm^2. All data below are presented without taking into account the heat losses and heat spreading.

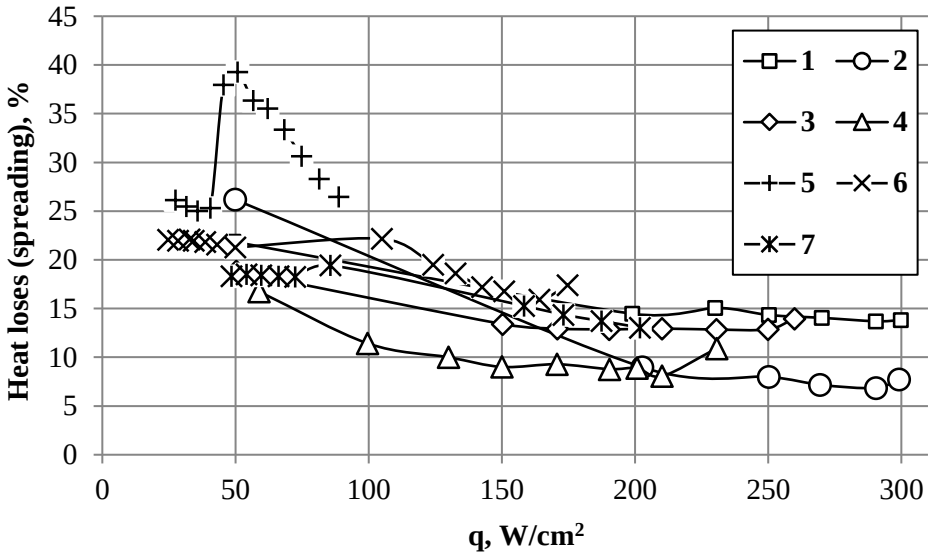

Figure 2. The heat loses into the atmosphere at Re_l = 19, H = 1.5 mm: 1 – U_{Sg} = 31 m/s; 2 – U_{Sg} = 28 m/s; 3 – U_{Sg} = 14 m/s; 4 – U_{Sg} = 6 m/s. The heat spreading into the steel plate at U_{Sg} = 11 m/s, H = 2 mm: 5 – Re_l = 15; 6 – Re_l = 22; 7 – Re_l = 32.

Figure 3 shows the distributions of the working surface temperature at the different heat fluxes using the measurements of thermocouples embedded into the test section. From the graph, it is seen that the construction of the test section provides a local heating.

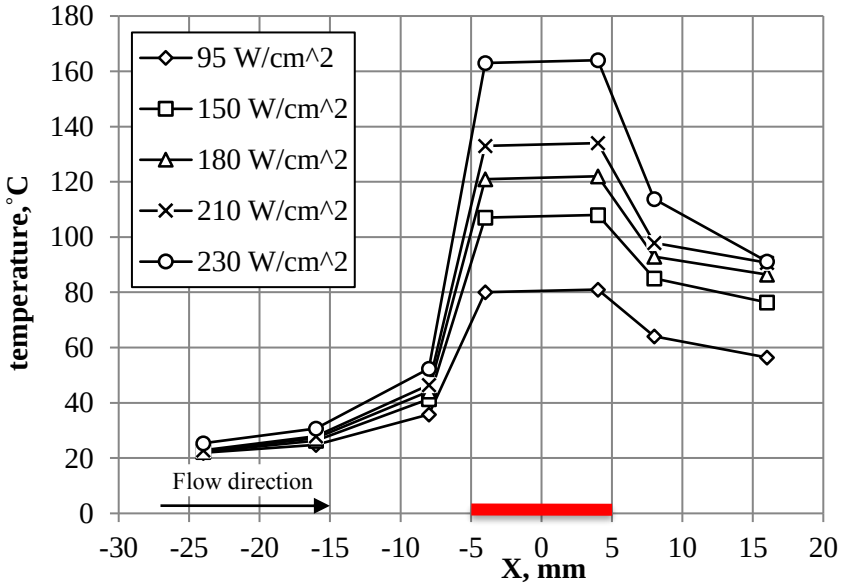

Figure 3. The distribution of the working surface temperature for different heat fluxes at U_{Sg} = 5 m/s and Re_l = 18, H = 0,25 mm. Red line shows the position of the heater.

3. Film rupture and CHF under local heating

Behaviour of the liquid film under local heating was investigated at H = 0.25, 0.5, 1, 1.2, 1.5 and 2 mm, in the ranges of q = 0-540 W/cm^2, Re_l = 8.5-50, Re_g = 350-2600, U_{Sg} = 3.8-40 m/s. Figure 4 illustrates the process of film disruption with increase of the heat flux at H = 0.5 mm, Re_l = 18, Re_g = 299 (U_{Sg} = 9.3 m/s). At a certain threshold heat flux q_{idp} the film ruptures with formation of a dry patch on the substrate. As usual, first dry patches initiate downstream of the heater along its lateral edges, as depicted in figure 4a. We deal with thermocapillary film rupture. Thermocapillary tangential stresses at the film surface, induced by the dependence of the liquid surface tension on the temperature, and tangential stresses, induced by the flowing gas, are the main competitive forces [12]. The film is thinnest along the lateral edges of the heater where temperature gradient at the film surface attains its maximum values. Film rupture is most likely to occur in this area. At a slightly higher heat flux $q_{idp,H}$ dry patches reach the heater (for smaller Re_g and smaller Re_l $q_{idp,H} = q_{idp}$). With further increase of the heat flux the heater is covered with metastable, intensively evaporating thin liquid film, with quickly emerging and disappearing small dry patches, figure 4b. And finally at the critical heat flux q_{cr}, the heater is suddenly dried out and its temperature starts to rise rapidly, figure 4c.

a) q = 100 W/cm^2, T_w = 83°C b) q = 250 W/cm^2, T_w = 140°C c) q = q_{cr} = 310 W/cm^2, crisis

Figure 4. Film rupture and crisis in shear-driven water film, heater 1x1 cm, H=0.5 mm, Re_l = 18, Re_g = 299 (U_{Sg} = 9.3 m/s), flow directed from top to bottom.

Figure 5 shows the effect of superficial gas velocity on the threshold heat flux for film rupture and on CHF, at Re_l = 14, and also the data for falling liquid film are presented (at Re_l = 14 $q_{idp} = q_{idp,H} = q_{cr}$). It is seen that at relatively small U_{Sg}, $q_{idp,H}$ and q_{cr} for shear-driven liquid film are close to those for falling liquid film. However at higher gas velocities, $q_{idp,H}$ for shear-driven liquid film is up to 3 times higher, while q_{cr}, almost linearly growing with U_{Sg}, at U_{Sg}=34 m/s is more than 10 times higher and reaches 250 W/cm^2. For shear-driven liquid film at increase of gas velocity, inertial force starts to dominate acting against thermocapillary forces, which provides more uniform liquid distribution over the heater as compared to gravity-driven liquid film. As a result, q_{cr} can be several times higher than q_{idp} and $q_{idp,H}$.

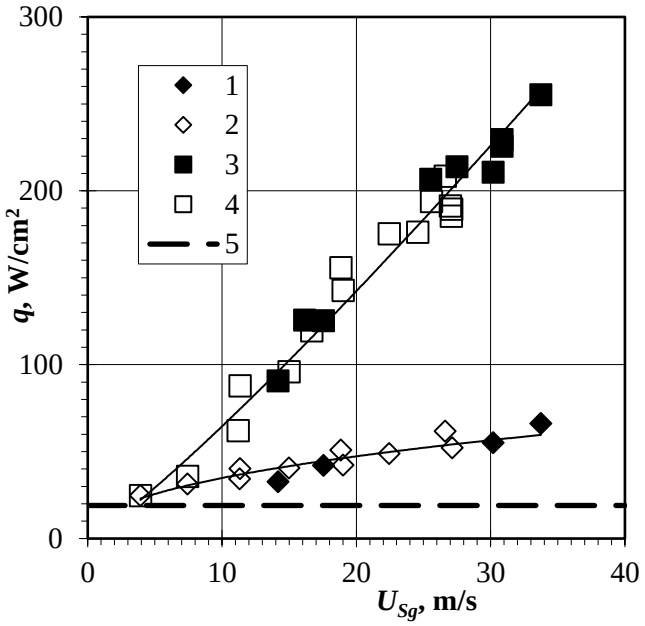

Figure 5. Effect of superficial gas velocity on film rupture and CHF, water-air flow, Re_l = 14. 1 – $q_{idp,H}$ at H = 1.2 mm; 2 – $q_{idp,H}$ at H = 1.5 mm; 3 – q_{cr} at H = 1.2 mm; 4 – q_{cr} at H = 1.5 mm; 5 – q_{idp} = $q_{idp,H}$ = q_{cr} for a falling liquid film. Curves, generalizing data for q_{idp}, $q_{idp,H}$ and q_{cr} are plotted.

Figure 6 shows the effect of gas velocity on CHF for a shear-driven liquid film for different Re_l and different H. It is seen that CHF grows with increase of both U_{Sg} and Re_l. In experiments the record value of CHF = 540 W/cm^2 was reached (point Re_l = 50, H=1 mm, U_{Sg} = 37 m/s). Unfortunately, the construction of the heater did not allow to achieve higher heat flux.

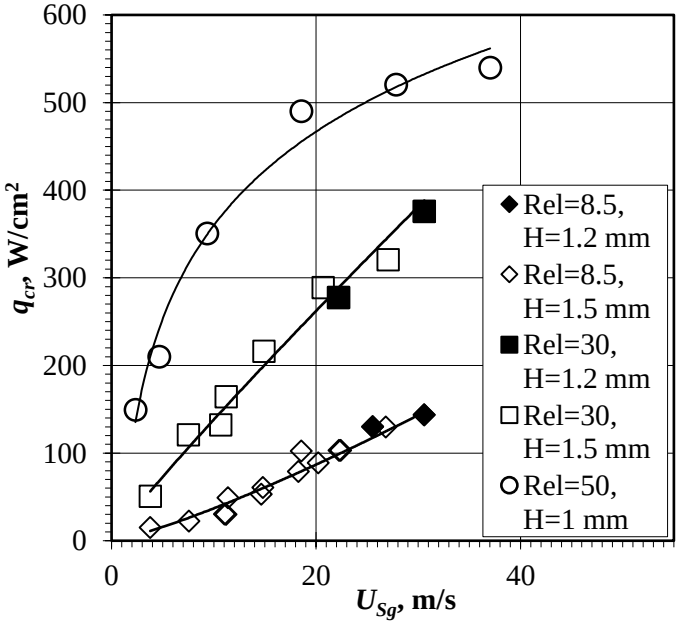

Figure 6. Effect of gas velocity on CHF for different liquid flow rates and different channel heights, water-air flow, horizontal channel, heater 1x1 cm. Curves, generalizing data are plotted for each Re_l.

4. Conclusions

From figures 5 and 6 it is seen that the channel height has no or little effect on CHF (within the range H=1.2-2.0 mm). For shear-driven water films the critical heat flux was found to be up to 10 times higher than that for a falling liquid film, and reaches up to 540 W/cm^2, which makes shear driven films (stratified and annular two-phase flow) very promising for high heat flux cooling applications. The heat loses into the atmosphere and heat spreading into the substrate in total don't exceed 30% at heat fluxes higher than 200 W/cm^2.

Acknowledgments

This work was supported by the Ministry of Education and Science of Russia (Agreement No 14.604.21.0053, project identifier RFMEFI60414X0053).

References

[1] Bar-Cohen A and Wang P 2012 Journal of Heat Transfer 134 (5) 051017-28
[2] Kabov O A, Lyulin Yu V, Marchuk I V and Zaitsev D V 2007 International Journal of Heat and Fluid Flow 28 103-112
[3] Gatapova E Ya and Kabov O A 2008 International Journal of Heat and Mass Transfer 51 (19) 4797-4810
[4] Goncharova O N and Kabov O A 2010 International Journal of Heat and Mass Transfer 53 (13-14) 2795-2807
[5] Kabova Y, Kabov O, Gambaryan-Roisman T, Stephan P and Kuznetsov V V 2014 International Journal of Heat and Mass Transfer 68 527-541
[6] Zaitsev D V, Rodionov D A and Kabov O A 2009 Technical Physics Letters 35 (7) 680-682
[7] Kabov O A and Zaitsev D V 2009 Multiphase Science and Technology 21 (3) 249-266
[8] Kabov O A, Chinnov E A and V Cheverda 2007 Microgravity Science and Technology 19 (3-4) 44-47
[9] Ajaev V S 2013 Interfacial Phenomena and Heat Transfer, 1 (1) 81-92
[10] Peles Y 2012 Contemporary Perspectives on Flow Boiling Instabilities in Microchannels and Minichannels (New York: Begell House) p 152
[11] Kadoura M and Chandra S 2013 Experiments in Fluids 54 (2) 1-11
[12] Chinnov E A and Kabov O A 2007 Microgravity Science and Technology. 19 (3-4) 18-22